HHS Public Access

Author manuscript

Gynecol Oncol. Author manuscript; available in PMC 2016 October 01.

Published in final edited form as:

Gynecol Oncol. 2015 October ; 139(1): 97–103. doi:10.1016/j.ygyno.2015.08.017.

Beyond genomics: critical evaluation of cell line utility for ovarian cancer research

Kevin M. Elias[*,1,2,3], **Megan M. Emori**[*,1,4], **Eniko Papp**[5], **Emily MacDuffie**[1], **Gottfried E. Konecny**[6], **Victor E. Velculescu**[5], and **Ronny Drapkin**[†,1,3,7]

[1]Dana-Farber Cancer Institute, Boston, MA 02115 USA

[2]Division of Gynecologic Oncology, Department of Obstetrics and Gynecology and Reproductive Biology, Brigham and Women's Hospital, Boston, MA 02115 USA

[3]Harvard Medical School, Boston, MA 02115 USA

[4]Graduate School of Arts and Sciences, Harvard University, Cambridge, MA 02138

[5]The Sidney Kimmel Comprehensive Cancer Center, Johns Hopkins University School of Medicine, Baltimore, MD 21287 USA

[6]University of California Los Angeles, Jonsson Comprehensive Cancer Center, Los Angeles, CA 90095

Abstract

Objective—Comparisons of The Cancer Genome Atlas (TCGA) with high grade serous ovarian cancer (HGSOC) cell lines used in research reveal that many common experimental models lack defining genomic characteristics seen in patient tumors. As cell lines exist with higher genomic fidelity to TCGA, this study aimed to evaluate the utility of these cell lines as tools for preclinical investigation.

Methods—We compared two HGSOC cell lines with supposed high genomic fidelity to TCGA, KURAMOCHI and OVSAHO, with the most commonly cited ovarian cancer cell line, SKOV3, which has poor genomic fidelity to TCGA. The lines were analyzed for genomic alterations, *in vitro* performance, and growth in murine xenografts.

[†]Correspondence to: Ronny Drapkin, Penn Ovarian Cancer Research Center, Department of Obstetrics and Gynecology, Perelman School of Medicine, University of Pennsylvania, Biomedical Research Building II/III, Rm. 1215, 421 Curie Blvd., Philadelphia, PA 19104, Telephone: 215.746.3973, rdrapkin@mail.med.upenn.edu.

[7]Present address: Penn Ovarian Cancer Research Center, Department of Obstetrics and Gynecology, Perelman School of Medicine, University of Pennsylvania, Philadelphia, PA 19104 USA

[*]Denotes equal contribution

Conflict of Interest Statement

RD is a member of the scientific advisory board of Siamab Therapeutics. KME is a member of the scientific advisory board of Firefly Bioworks, Inc. VEV is a member of the board of directors and scientific advisory board of Personal Genome Diagnostics. The remaining authors disclose no potential conflicts.

Results—Using targeted next generation sequencing analyses, we determined that each line had a distinct mutation profile, including alterations in *TP53*, and copy number variation of specific genes. KURAMOCHI and OVSAHO better recapitulated serous carcinoma morphology than SKOV3. All lines expressed PAX8 and stathmin, but KURAMOCHI and OVSAHO did not express CK7. KURAMOCHI was significantly more platinum sensitive than OVSAHO and SKOV3. Unlike SKOV3, KURAMOCHI and OVSAHO engrafted poorly in subcutaneous xenografts. KURAMOCHI and OVSAHO grew best after intraperitoneal injection in SCID mice and recapitulated miliary disease while SKOV3 grew in all murine systems and formed oligometastatic disease.

Conclusions—The research utility of HGSOC cell line models requires a comprehensive assessment of genomic as well as *in vitro* and *in vivo* properties. Cell lines with closer genomic fidelity to human tumors may have limitations in performance for preclinical investigation.

Introduction

Experimentation using cancer cell lines remains among the most commonly used laboratory approaches in oncology research. While much attention has been paid to patient-derived xenografts (PDXs), established cancer cell lines available from commercial or academic repositories are the backbone of basic scientific investigation [1,2]. Traditional cell lines have several advantages over primary cell lines: 1) equal access for investigators from around the world; 2) a high propensity to be cultured indefinitely without senescence; 3) a large degree of publicly available genomic data regarding the lines from the Broad-Novartis Cancer Cell Line Encyclopedia (CCLE) and Wellcome Trust Sanger Institute Catalogue of Somatic Mutations in Cancer (COSMIC) Cell Lines Project; and 4) few barriers to material transfer among collaborating institutions [3,4].

In the ovarian cancer research community, however, years of working with traditional cell lines was upended in many respects by the recent availability of the high grade serous ovarian cancer (HGSOC) dataset from The Cancer Genome Atlas (TCGA) [5]. Subsequent reports by Domcke, *et al* and Anglesio, *et al* compared the genomes of cell lines to the genomes of actual patient tissue samples from TCGA and demonstrated that the most highly utilized HGSOC cell lines poorly represented the genomic features of the majority of human ovarian cancers [6,7]. These lines, most notably SKOV3 and A2780, have become common place because they form discrete tumors whether injected orthotopically or ectopically into nude mice and are easily manipulated using transfection techniques [8–11]. However, without the defining genomic alterations seen in most patient samples, the utility of these cell lines is now in question.

We hypothesize that the movement of the research community to embrace new cancer cell lines will require careful consideration of their performance in laboratory systems and perhaps tradeoffs in current approaches to conventional research. As a proof of concept, we describe a series of genomic, *in vitro*, and *in vivo* analyses we used to characterize two cell lines, OVSAHO and KURAMOCHI, proposed by Domcke, *et al* as having higher genomic fidelity to TCGA. We compare the research utility of these lines to SKOV3 and offer our approach as a model strategy for evaluating future cell lines for cancer research.

Methods

Cell Culture

SKOV3, IGROV1, OVCAR3, OVCAR4, OVCAR8, and MCF7 cells were purchased from ATCC (Manassas, VA). KURAMOCHI, OVSAHO, and JHOS4 cells were a gift from Dr. Gottfried Konecny (UCLA, Los Angeles, CA). All cancer cell lines were cultured in DMEM:F12 media (Mediatech, Inc, Manassas, VA) supplemented with 10% fetal bovine serum (Atlanta Biologicals, Norcross, GA) and 1% penicillin/streptomycin (Gibco, Life Technologies, Grand Island, NY). FT194 cells were derived from human fallopian tube secretory cells as previously described, and cells were cultured in DMEM:F12 supplemented with 2% Ultraser™ G (Pall Corporation, Port Washington, NY) and 1% penicillin/streptomycin [12]. All cells were incubated at 37°C with 5% CO_2.

Specimens Obtained for Sequencing Analysis

The identities of the cell lines SKOV3, OVSAHO, and KURAMOCHI were authenticated by typing 10 short tandem repeat (STR) loci using the PowerPlex 2.1 System (Promega, Madison, WI). Normal samples were obtained from 10 unmatched lymphoblast cultures (Coriell Institute for Medical Research, Camden, NJ).

Massively Parallel Paired-End Sequencing and Somatic Mutation Identification

Sample library construction, targeted capture, next generation sequencing, and bioinformatic analyses of cell lines were performed as previously described [13]. In brief, fragmented genomic DNA from cell lines was used for analysis of targeted regions using custom Agilent Sure Select probes according to the manufacturer's instructions (Agilent, Santa Clara, CA). Captured DNA libraries were sequenced with the Illumina MiSeq System (Illumina, San Diego, CA). Sequence reads were analyzed and aligned to the human genome sequence (hg18) with the Eland v.2 algorithm in CASAVA 1.7 software (Illumina, San Diego, CA). Potential somatic mutations and copy number alterations were identified as previously described [13, 14]. As the analyzed cell lines lacked matched normal controls, additional filters were applied. Mutations present in an unmatched normal sample, sequenced to a similar coverage and on the same platform as the matched normal, were removed. Additionally, alterations reported in the 1000 Genomes project, present in >1% of the population, or listed as Common in dbSNP138 were also removed.

siRNA

RNAi knockdown was performed by reverse transfection using three different pre-designed siRNA oligonulceotides (catalogue numbers s15403, s15404, and s15405, abbreviated 403, 404, and 405, respectively, Ambion, Life Technologies, Grand Island, NY)or pooled siRNA targeting PAX8 or control siRNA oligonucleotides targeting no known mammalian genes. Oligonucleotides were diluted in Opti-MEM I medium (Gibco, Life Technologies, Grand Island, NY) without serum and then assembled into RNAi transfection complexes by incubating with RNAiMAX Lipofectamine (Life Technologies, Grand Island, NY) for 10 minutes. Aliquots of cells diluted in Opti-MEM I medium were then added to the RNAi complexes. One aliquot of cells received no siRNA complexes and served as a no

transfection control. All cells were incubated for 72 hours before lysates were created to assess knockdown.

Western Blots

Whole cell extracts were created by lysing cell pellets with RIPA buffer (Boston BioProducts, Ashland, MA) for 20 min on ice, and then lysates were cleared by centrifugation for 10 minutes at 15,000 rpm at 4°C. Samples were loaded onto NuPage 4–12% Bis-Tris gradient gels (Novex, Life Technologies, Grand Island, NY) and separated by electrophoresis in MOPS-SDS running buffer. Proteins were transferred to nitrocellulose membranes via the iBlot dry transfer system (Invitrogen, Life Technologies, Grand Island, NY). Blots were blocked for 1 hour at room temperature in 5% nonfat milk in PBS-Tween-20 (Westnet Inc., Canton, MA) and incubated in appropriate primary antibodies diluted in blocking buffer overnight at 4°C (Supplemental Table S1). Blots were then incubated in HRP-linked secondary antibody (GE Healthcare, Piscataway, NJ) at 1:4,000 dilution in blocking buffer. Proteins were detected using the ECL2 western blotting substrate kit (Thermo Fisher Scientific, Waltham, MA) and imaged with a FluorChem HD2 imager (Cell Biosciences, Santa Clara, CA). After initial development, membranes were re-probed with antibodies to β-actin (Sigma-Aldrich, St. Louis, MO) as a loading control.

Luciferization of Cell Lines

Cell lines were plated at 50,000 cells per well on 6 well tissue culture plates in complete media. The next day, the media was aspirated and lentiviral particles containing an mCherry-luc construct (a gift from Dr. Sangeetha Palakurthi, Dana-Farber Cancer Institute Belfer Center, used with permission from Dr. Andrew Kung, Columbia University) were added at a range of multiples of infection (MOI) with 8 ug/mL Hexadimethrine Bromide (Polybrene, Sigma-Aldrich, St. Louis, MO) [15]. The virus containing media was removed and replaced with regular complete media the next day. After another 24 hours of culture, 0.5 ug/mL puromycin (Sigma-Aldrich, St. Louis, MO) was added to all wells to induce selection. Cells were continued under negative selection using puromycin with media changes every 72 hours until all cells had died in the uninfected control wells. Surviving cells were then positively selected using flow cytometry to purify the mCherry expressing cells. The mCherry-positive cell lines were then expanded in culture and periodically checked for purity using fluorescence microscopy. The correlation between cell number and luciferase activity was determined by creating serial dilutions of each cell line and then measuring luciferase activity, quantified via the ONE-Glo™ Luciferase Assay System (Promega, Madison, WI) on a Modulus™ microplate reader (Promega, Madison, WI). Cell number and luciferase activity were linearly correlated for all lines (Figure S1).

Platinum Sensitivity Assay

Luciferized KURAMOCHI, OVSAHO, and SKOV3 cells were plated at 2,500 cells per well in sextuplicate on a 96 well plate and treated with *cis*-diamminedichloroplatinum (II) (cisplatin, Sigma-Aldrich, St. Louis, MO) at indicated concentrations in complete media. Cells were incubated for 96 hours, and cell number was quantified by luciferase activity.

Xenografts

All animal protocols were approved by the Institutional Animal Care and Use Committee (IACUC) at Dana-Farber Cancer Institute. Prior to experiments in mice, all cell lines were screened for mycobacteria and viruses via Mouse Antibody Production (MAP) testing (Charles River Research Animal Diagnostic Services, Wilmington, MA) and found to be pathogen free. All mice were obtained from the Jackson Laboratory (Bar Harbor, ME). Mice were monitored in accordance with IACUC guidelines and given food and water ad libitum. Mice were weighed weekly and assessed for body conditioning scores. Volumetric tumor growth in the subcutaneously injected mice was measured weekly in two dimensions using calipers.

Imaging

Mice were temporarily anesthetized with isoflurane and injected either intraperitoneally (i.p) or subcutaneously (s.c.) with luciferin (Gold Biotechnology, St. Louis, MO) based on tumor location. 5–10 minutes later, mice were imaged using an IVIS® in vivo imaging system (PerkinElmer, Shelton, CT). Images were taken at F-stop1 and medium binning with a series of exposures. Post-image processing and quantification was performed in Living Image® (PerkinElmer, Shelton, CT) where intensity scales were normalized across time points for each cell line and region of interest (ROI) measured. Tumor volumes were calculated from two dimension measurements using the formula $0.5 \times (\text{length} \times \text{width}^2)$ as described [16, 17].

Histology

After euthanasia, necropsies were immediately performed, and tissues were placed in cassettes. Tissues were fixed for 24 hours at room temperature in 10% neutral buffered formalin, then transferred to 70% ethanol. Tissues were embedded in paraffin blocks, and then histologic sections were stained with hematoxylin and eosin.

Immunohistochemistry

Immunohistochemistry of paraffin embedded sections was performed using the Envision Plus/Horseradish Peroxidase system (Dako, Carpinteria, CA). Primary polyclonal antibodies were used toPAX8 (Proteintech, Chicago, IL, Catalog # 10336-1-AP, 1:1000 dilution), WT-1 (Abcam, Cambridge, UK, Catalog # ab89901, 1:250 dilution), and p53 (Epitomics, Cambridge, MA, Catalog #1026-1, 1:300 dilution). Antigen retrieval for all targets was performed using pressure cooker pretreatment in citrate buffer (pH=6.0). Appropriate positive (PAX8, thryoid; WT-1, mesothelioma; p53, colon)) and negative (incubation with secondary antibody only) controls were stained in parallel for each round of immunohistochemistry. Strong nuclear staining for each epitope was considered positive.

Statistical Analysis

For the platinum sensitivity assay, log dose response curves were constructed, and the mean IC50 values compared using the extra sum-of-squares F test (GraphPad, San Diego, CA). A p-value of less than 0.05 was considered significant.

Results

Genomic properties

Our targeted genomic analysis of 113 genes revealed that SKOV3 had twenty-five sequence mutations in genes with known functional roles in human cancer, whereas OVSAHO had only five mutations and KURAMOCHI had only six mutations (Table 1). The only gene that was commonly mutated in all three cell lines was *TP53*, although mutations were found in *NF1* in both SKOV3 and OVSAHO and in *ATM* in both SKOV3 and KURAMOCHI. Through analyses of copy number variation, we identified a deletion in *CDKN2A* and amplification of *ERBB2* in SKOV3 whereas OVSAHO had an amplification in *FGFR4* and KURAMOCHI had amplifications of *KRAS* and *MYC* (Table 2).

In vitro properties

On tissue culture plates, KURAMOCHI cells assembled into classic cobblestone appearing carcinoma sheets with prominent nucleoli and marked cytologic atypia, while OVSAHO cells formed small rosettes and micropapillary structures (Figure 1A). This is in marked contrast to SKOV3 cells, which assumed a spindle shape with dendritic-like projections. KURAMOCHI and OVSAHO expressed common markers of HGSOC, including PAX8 and stathmin but surprisingly did not express CK7 (Figure 1B). This was not due to a mutation, as determined by DNA sequencing (data not shown). By western blot, KURAMOCHI showed accumulation of the mutated form of p53. Confirming the genomic results, OVSAHO had a truncated form of p53 that resulted in a lower molecular weight product, and SKOV3 did not express detectable p53 protein due to its truncating deletion (Figure 1B). Using PAX8 as a target, we found all three cell lines were easily transfected with siRNA with comparable levels of protein knockdown to that observed in several well-annotated cell lines (Figure 1C). KURAMOCHI was significantly more sensitive to cisplatin than SKOV3, whereas OVSAHO and SKOV3 had nearly identical IC50 values (Figure 2).

Tumor growth in mice

Most xenograft models for HGSOC use the SKOV3 cancer line injected into athymic (nude) mice. Consequently, we first studied the properties of KURAMOCHI and OVSAHO in this model. We also tested another high grade serous carcinoma cell line described by Domcke, *et al* called JHOS4. To allow observation of tumor growth kinetics, we stably introduced a luciferase reporter that provides bioluminescent imaging into SKOV3, KURAMOCHI, OVSAHO, and JHOS4 using a lentivirus containing the mCherry-Luc construct. We injected 2.5 million cells i.p. into each experimental mouse and used a non-injection control in each cage that received only vehicle. At 13 days post-injection, tumors were easily detected in all experimental mice (Figure S2). While tumors remained easily detectable for xenografts with the SKOV3 and KURAMOCHI lines at 27 days post-injection, the OVSAHO tumors appeared to be growing more slowly than the other two cell lines. We continued to observe the OVSAHO and JHOS4 tumors *in vivo* until 46 days post-injection. With extended observation, however, the tumors did not grow larger and in some cases even seemed to regress. At the time of necropsy, grossly visible tumors were not identifiable for OVSAHO in any mouse. The JHOS4 cell line grew especially poorly in the athymic xenografts; consequently we did not continue to use this line in subsequent experiments.

Although nude mice have compromised cell-mediated immunity due to the absence of T cells, they do still have NK cells, an intact innate immune system, and humoral immunity via B cells. We hypothesized that tumor growth might improve by using NOD scid gamma (NSG) mice, which lack all mature lymphocytes and have extremely low natural killer (NK) cell activity. We also increased the tumor inoculation burden to 5 million cells per mouse and injected mice either i.p. or s.c. to allow for maximal flexibility in measuring tumor growth and harvesting clearly defined tumor masses.

As expected, the s.c. injections allowed for very precise monitoring of the tumor size in each mouse (Figure 3A). The bioluminescent imaging technique was much more sensitive for detecting tumors than palpation or caliper measurement (Figure S3A and B). While the SKOV3 tumors grew steadily up to 200 mm^3, the KURAMOCHI tumors halted growth at a tumor size of about 12 mm^3, and the OVSAHO tumors were barely perceptible. Histologically, SKOV3 formed large expansile tumors, whereas KURAMOCHI formed distinct nodules, and OVSAHO formed microscopic tumors but with a marked desmoplastic response (Figure 3B–C).

All tumors grew more efficiently in the i.p. NSG model. SKOV3 formed large discrete tumors that mimicked oligometastatic disease (Figure 4A). KURAMOCHI and OVSAHO created tiny visceral and peritoneal implants, more consistent with miliary disease, and were better mimics of carcinomatosis. OVSAHO failed to implant in one mouse. None of the cell lines created ascites. While the KURAMOCHI tumors were larger and more easily identified grossly, OVSAHO produced more diffuse implants (Figure 4A). All three lines caused some mice to develop signs of early small bowel obstructions. Histologically, SKOV3 tumors were large discrete tumor masses, whereas KURAMOCHI and OVSAHO were more commonly found as peritoneal implants or invading into viscera (Figure 4B). As the most common clinical immunohistochemical stains used to identify high grade serous tumors are PAX8, WT1, and p53, we also stained the xenografts for these markers. All three tumors stained for PAX8. In SKOV3, the WT1 staining was nucleolar only, while KURAMOCHI and OVSAHO had strong nuclear staining for WT1. Consistent with the finding of a deletion in *TP53* in our genomic analysis, SKOV3 tumors did not show accumulation of p53, whereas KURAMOCHI and OVSAHO demonstrated strong staining.

Discussion

Ovarian cancer remains the most lethal gynecologic malignancy for American women [18]. Despite decades of intense laboratory research into novel treatments for this disease, there has been minimal improvement in overall survival for patients [19]. The disconnect between seemingly robust treatments in preclinical studies and actual early phase clinical trial outcomes may stem from the fact that the most commonly used laboratory models are in many respects poor phenocopies of the human disease.

In this study we sought to describe an approach for assessing the experimental utility of cell lines with apparent higher genomic fidelity to patient tumors by comparing the most commonly used cell line in HGSOC preclinical studies, SKOV3, with two less well-described cell lines, KURAMOCHI and OVSAHO. The work by Domcke, *et al* noted these

latter lines are more genomically akin to the tumors in TCGA. All three lines expressed the two most important markers for HGSOC, PAX8 and mutated p53. Notably, the deletion in *TP53* we observed in SKOV3 was not reported by Domcke, *et* al. This may be due to several existing clones of SKOV3 which are in use among laboratories; our sequencing data were from SKOV3-cis, which is a cisplatin resistant daughter cell line of SKOV3. The other mutations we identified in SKOV3 matched those seen by Domcke, *et al;* perhaps this is related to cisplatin resistance, or is simply an additional driver that occurred in this clone. While the absence of commonly mutated driver genes that we observed is typical of HGSOC, our targeted genomic analysis did not capture the significant copy number variation that is the signature of this disease. Whole genome analysis has previously estimated that KURAMOCHI and OVSAHO have 54% and 43% of their genome altered by copy number variation, respectively, while copy number changes are much lower in SKOV3 with only 14% of the genome impacted by copy number variation [6].

In vitro, we found these newer cell lines, like SKOV3, were relatively easy to culture and useful for common ovarian cancer research techniques like platinum sensitivity assays and RNAi knockdown. KURAMOCHI was the most platinum sensitive of the three lines, likely due to a mutation in BRCA2 [6]. *In vivo* however, we discovered that unlike SKOV3, KURAMOCHI and OVSAHO do not grow well in nude mice or when implanted subcutaneously. This is in keeping with the recent work by Mitra, *et al* in this journal which also looked at tumor growth in nude mice [20]. To that work we have added the finding that these tumors can be grown in NSG mice. Additionally, KURAMOCHI and OVSAHO form small peritoneal tumor implants, which reflect miliary disease. While this pattern of spread is more common clinically than the oligometastatic pattern displayed by SKOV3, it requires considerably more skill to identify tumors both grossly and during sectioning. Moreover, KURAMOCHI and OVSAHO grew more slowly *in vivo* than SKOV3, with more variability from mouse to mouse.

Taken together, our data illustrate the challenges that must be overcome not only for working with KURAMOCHI and OVSAHO, but more generally with any new HGSOC cell lines. All cell lines must be genomically profiled and characterized *in vitro.* However, *in vitro* characteristics may not predict *in vivo* performance. To maximize tumor formation, we suggest using NSG mice over nude mice. Tumors should be injected intraperitoneally to allow for metastatic spread. We recommend that tumor lines be luciferized to allow for bioluminescent imaging and an accurate assessment of growth kinetics. Finally, during histologic analysis, apparent tumor implants should be confirmed by immunohistochemistry using antibodies directed against PAX8, WT1, and p53– the same marker used in clinical practice to identify Mullerian malignancies.

In conclusion, the emerging genomic data on high grade serous ovarian cancers have forced a long overdue reappraisal of laboratory models of this disease. Investigators should be using cell lines that reflect the molecular, anatomic, and clinical dimensions of patient disease. While specific cancer cell lines may be reflective of small subsets of patients, it can no longer be considered scientifically valid to apply preclinical experimental conclusions to the majority of patients using cell lines that reflect a very small minority of individuals. Unfortunately, working with these newer cell lines requires considerably more time and

expense than prior models. Researchers also need to develop new cell lines selected specifically to cover the wide range of ovarian cancer subtypes. The reward for this investment, however, is likely to be preclinical data more likely to translate into actual treatments for patients.

Supplementary Material

Refer to Web version on PubMed Central for supplementary material.

Acknowledgments

Funding

This work was supported by the Ruth N. White Research Fellowship in Gynecologic Oncology(KME), the Sperling Family Fund Fellowship(KME), the Robert and Deborah First Fund(KME, RD), the Ruth L. Kirschstein National Research Service Award F31-CA176995-01A1 (MME), the National Cancer Institute at the NIH P50-CA083636 (RD), NIH U01-CA152990 (RD), NIH R21-CA156021 (RD), CA121113 (VEV), the Dr. Miriam and Sheldon G. Adelson Medical Research Foundation (RD, VEV, GK), the Honorable Tina Brozman Foundation (RD), and the Gamel Family Ovarian Cancer Research Fund (RD), and the Commonwealth Foundation (VEV).

References

1. Weroha SJ, Becker MA, Enderica-Gonzalez S, et al. Tumorgrafts as in vivo surrogates for women with ovarian cancer. Clin Cancer Res. 2014; 20(5):1288–97. [PubMed: 24398046]
2. Scott CL, Becker MA, Haluska P, Samimi G. Patient-Derived Xenograft Models to Improve Targeted Therapy in Epithelial Ovarian Cancer Treatment. Front Oncol. 2013; 3:295. [PubMed: 24363999]
3. Barretina J, Caponigro G, Stransky N, et al. The Cancer Cell Line Encyclopedia enables predictive modeling of anticancer drug sensitivity. Nature. 2012; 483(7391):603–7. [PubMed: 22460905]
4. Forbes SA, Beare D, Gunasekaran P, et al. COSMIC: exploring the world's knowledge of somatic mutations in human cancer. Nucl Acids Res. 2015; 43(Database issue):D805–11. Website: cancer.sanger.ac.uk.
5. Cancer Genome Atlas Research Network. Integrated genomic analyses of ovarian carcinoma. Nature. 2011; 474(7353):609–15. [PubMed: 21720365]
6. Domcke S, Sinha R, Levine DA, Sander C, Schultz N. Evaluating cell lines as tumour models by comparison of genomic profiles. Nat Commun. 2013; 4:2126. [PubMed: 23839242]
7. Anglesio MS, Wiegand KC, Melnyk N, et al. Type-specific cell line models for type-specific ovarian cancer research. PLoS One. 2013; 8(9):e72162. [PubMed: 24023729]
8. Xiang Y, Ma N, Wang D, et al. MiR-152 and miR-185 co-contribute to ovarian cancer cells cisplatin sensitivity by targeting DNMT1 directly: a novel epigenetic therapy independent of decitabine. Oncogene. 2014; 33(3):378–86. [PubMed: 23318422]
9. Selvendiran K, Ahmed S, Dayton A, et al. HO-3867, a synthetic compound, inhibits the migration and invasion of ovarian carcinoma cells through downregulation of fatty acid synthase and focal adhesion kinase. Mol Cancer Res. 2010; 8(9):1188–97. [PubMed: 20713491]
10. Gourley C, Paige AJ, Taylor KJ, et al. WWOX gene expression abolishes ovarian cancer tumorigenicity in vivo and decreases attachment to fibronectin via integrin alpha3. Cancer Res. 2009; 69(11):4835–42. [PubMed: 19458077]
11. Park YA, Lee JW, Kim HS, et al. Tumor suppressive effects of bromodomain-containing protein 7 (BRD7) in epithelial ovarian carcinoma. Clin Cancer Res. 2014; 20(3):565–75. [PubMed: 24198243]
12. Karst AM, Drapkin R. Primary culture and immortalization of human fallopian tube secretory epithelial cells. Nat Protoc. 2012; 7(9):1755–64. [PubMed: 22936217]

13. Sausen M, Leary RJ, Jones S, et al. Integrated genomic analyses identify ARID1A and ARID1B alterations in the childhood cancer neuroblastoma. Nat Genet. 2013 Jan; 45(1):12–7. [PubMed: 23202128]
14. Jones S, Anagnostou V, Lytle K, et al. Personalized genomic analyses for cancer mutation discovery and interpretation. Sci Transl Med. 2015 Apr 15.7(283):283ra53.
15. Tseng JC, Kung AL. Quantitative bioluminescence imaging of mouse tumor models. Cold Spring Harb Protoc. 2015; 2015(1) pdb.prot078261.
16. Euhus DM, Hudd C, LaRegina MC, Johnson FE. Tumor measurement in the nude mouse. J Surg Oncol. 1986; 31(4):229–234. [PubMed: 3724177]
17. Tomayko MM, Reynolds CP. Determination of subcutaneous tumor size in athymic (nude) mice. Cancer Chemother Pharmacol. 1989; 24(3):148–154. [PubMed: 2544306]
18. Siegel RL, Miller KD, Jemal A. Cancer statistics, 2015. CA Cancer J Clin. 2015; 65(1):5–29. [PubMed: 25559415]
19. Allemani C, Weir HK, Carreira H, et al. Global surveillance of cancer survival 1995–2009: analysis of individual data for 25,676,887 patients from 279 population-based registries in 67 countries (CONCORD-2). Lancet. 2015; 385(9972):977–1010. [PubMed: 25467588]
20. Mitra A, Davis DA, Tomar S, Roy L, Gurler H, Xie J, et al. In vivo tumor growth of high-grade serous ovarian cancer cell lines. Gynecologic Oncology. 2015 Epub ahead of print.

Highlights

- Characterization of new ovarian cancer cell lines requires genomic, *in vitro*, and *in vivo* analyses.
- KURAMOCHI and OVSAHO are two cells lines which phenotypically recapitulate high grade serous ovarian cancer better than SKOV3.
- Optimal xenografts using KURAMOCHI and OVSAHO cells should use intraperitoneal injection of luciferized cells into NSG mice.

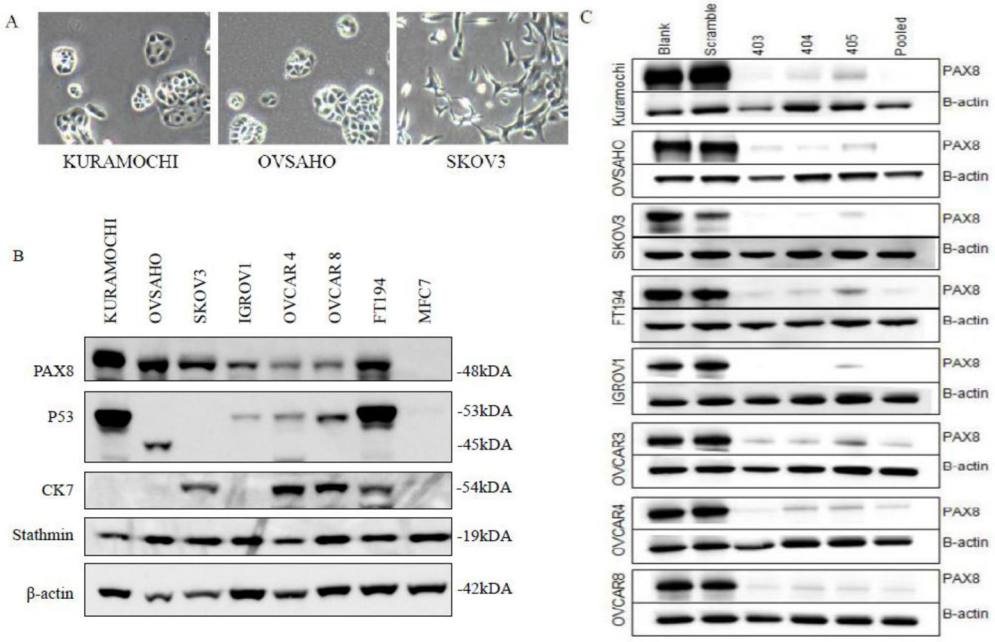

Figure 1.

In vitro properties of ovarian cancer cell lines. A) Light microscopy images of KURAMOCHI, OVASAHO, and SKOV3 in two-dimensional culture. All pictures 400x magnification. B) Western blots showing expression of characteristic high grade serous ovarian cancer proteins across several ovarian cancer cell lines as well as an immortalized normal fallopian tube cell line (FT194) and breast cancer cell line (MCF7). C) Western blots demonstrating efficiency of siRNA knockdown across various cell lines using PAX8 as a target. Shown are no transfection control (blank), a scramble non-targeting siRNA, three PAX8 targeting siRNA sequences (designated 403, 404 and 405), and a pooled targeted siRNA (encompassing all three targeted siRNA sequences).

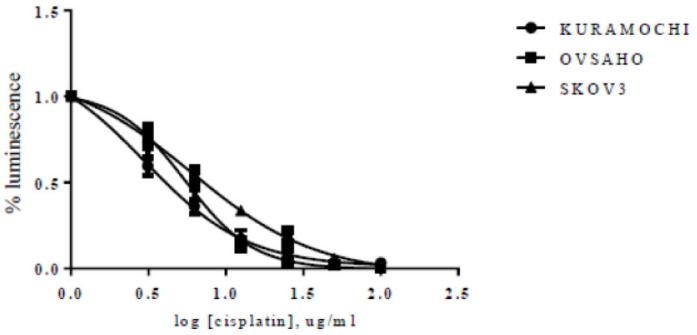

Cell Line	IC50	95% CI	p-value compared to SKOV3	p-value compared to OVSAHO
KURAMOCHI	3.001	2.321 - 3.881	0.0002	<0.0001
OVSAHO	5.450	4.794 - 6.196	0.49	--
SKOV3	5.986	5.075 – 7.059	--	0.49

IC = half maximal inhibitory concentration; CI = confidence interval

Figure 2.

Platinum sensitivity of cell lines. Cell number was assessed as relative luminescence compared to the untreated control for each cell line after 96 hours of cisplatin exposure across the indicated concentrations of drug. Curves represent the summary of 4 independent experiments.

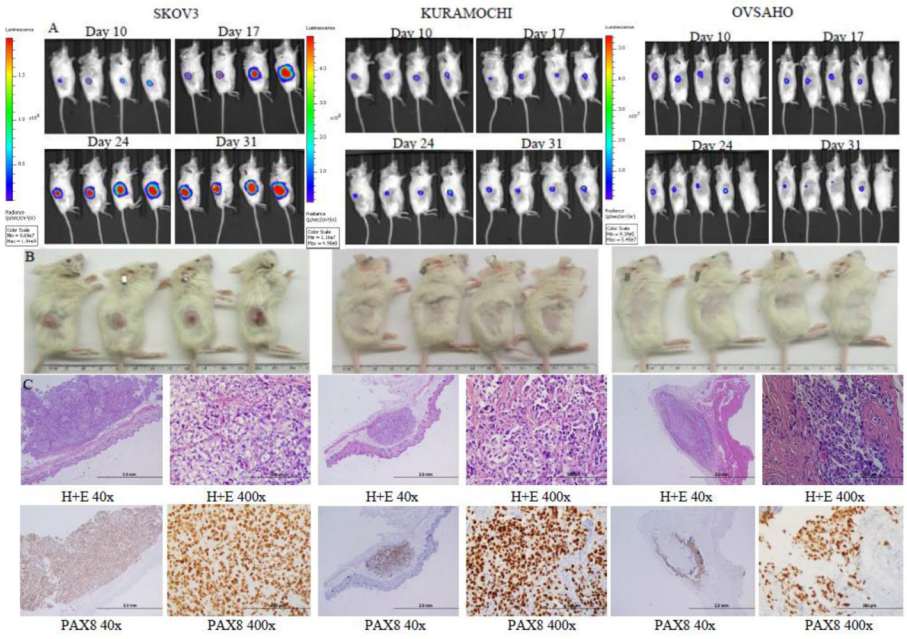

Figure 3.

Xenograft growth of cell lines after subcutaneous implantation. A) Tumor growth by bioluminescent imaging. B) Photographs of tumors after euthanasia. C) Light microscopy images of tumors at 40x and 400x magnification showing histology by hematoxylin and eosin staining and identification of tumor cells by PAX8 immunohistochemistry.

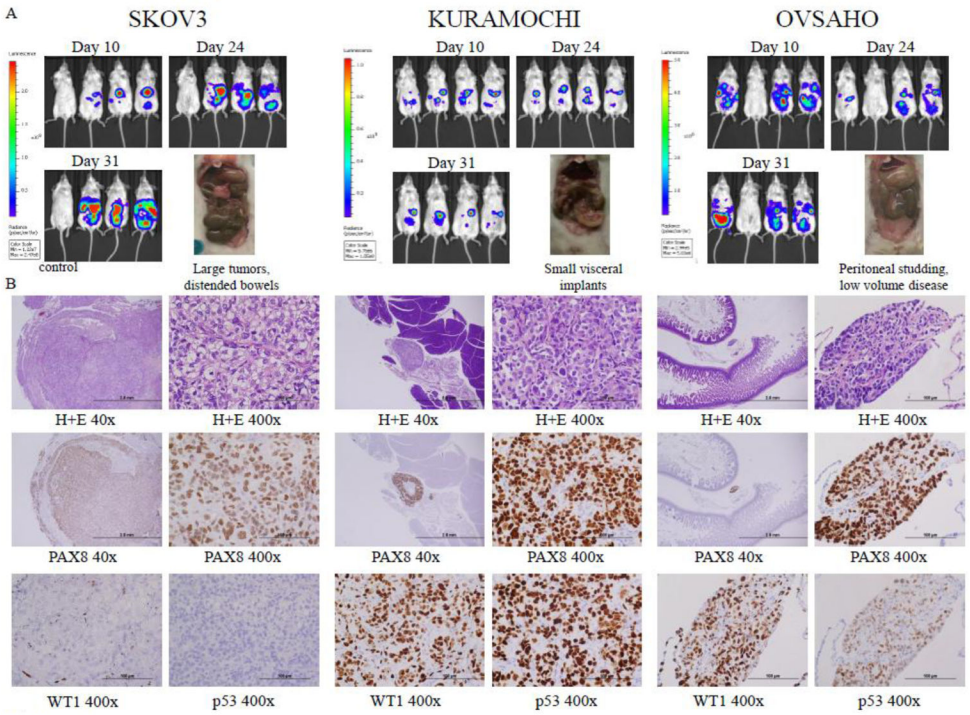

Figure 4.

Xenograft growth of cell lines after intraperitoneal implantation. A) Tumor growth by bioluminescent imaging and photographs of tumors at necropsy. B) Light microscopy images of tumors at 40x and 400x magnification showing histology by hematoxylin and eosin staining and identification of tumor cells by PAX8, WT1, and p53 immunohistochemistry.

Table 1

Sequence alterations identified in cell lines.

Cell Line	Gene ID	Amino Acid	Mutation Type	Consequence	Protein Domain
SKOV3	ABL1	964A>V	Substitution	Nonsynonymous coding	F-actin binding (953–1130)
	AKT1	293F>L	Substitution	Nonsynonymous coding	Serine/Threonine protein kinases, catalytic domain (150–408); Catalytic domain of the Protein Serine/ Threonine Kinase, Protein Kinase B (154–477)
	APC	2735G>R	Substitution	Nonsynonymous coding	EB-1 Binding Domain (2670–2843)
	ARID1A	658S>G	Substitution	Nonsynonymous coding	-
	ARID1A	1873P>H	Substitution	Nonsynonymous coding	-
	ARID1A	586Q>X	Substitution	Nonsense	-
	ARID1B	2177M>V	Substitution	Nonsynonymous coding	Domain of unknown function (DUF3518) (1926–2182)
	ATM	NA	Substitution	Splice site acceptor	-
	ERBB4	534E>G	Substitution	Nonsynonymous coding	Furin-like repeats (501–537)
	FGFR2	560P>H	Substitution	Nonsynonymous coding	Catalytic domain of the Protein Tyrosine Kinase, Fibroblast Growth Factor Receptor 2 (465–768); Protein tyrosine kinase (481–757)
	FLT3	450A>V	Substitution	Nonsynonymous coding	-
	FLT3	59S>A	Substitution	Nonsynonymous coding	-
	HNF1A	447P>S	Substitution	Nonsynonymous coding	Hepatocyte nuclear factor 1 (HNF-1), beta isoform C terminus (316–541)
	IGF1R	218T>M	Substitution	Nonsynonymous coding	Furin-like cysteine rich region (175–333)
	MLH1	NA	Large Indel	Large Indel	DNA mismatch repair protein MutL (6–315)
	NF1	1171K>M	Substitution	Nonsynonymous coding	-
	NF1	1702G>C	Substitution	Nonsynonymous coding	Sec14p-like lipid-binding domain (1560–1706)
	NOTCH2	NA	Deletion	Frameshift	-
	PAX5	111A>D	Substitution	Nonsynonymous coding	Paired Box domain (16–142); Paired Box domain (16–140)
	PIK3CA	1047H>R	Substitution	Nonsynonymous coding	Phosphoinositide 3-kinase (PI3K), class IA, alpha isoform, catalytic domain (699–1064)
	RB1	NA	Deletion	Frameshift	-
	ROS1	139L>V	Substitution	Nonsynonymous coding	-
	SMARCB1	9T>I	Substitution	Nonsynonymous coding	-
	STAG2	1124T>N	Substitution	Nonsynonymous coding	-
	TP53	NA	Deletion	Frameshift	-
OVSAHO	NF1	1720E>D	Substitution	Nonsynonymous coding	-

Cell Line	Gene ID	Amino Acid	Mutation Type	Consequence	Protein Domain
KURAMOCHI	PMS2	671T>M	Substitution	Nonsynonymous coding	-
	PMS2	485T>K	Substitution	Nonsynonymous coding	-
	TET2	457A>S	Substitution	Nonsynonymous coding	-
	TP53	342R>X	Substitution	Nonsense	P53 tetramerisation motif (319–359)
	ATM	1644M>T	Substitution	Nonsynonymous coding	-
	BRCA2	2318R>X	Substitution	Nonsense	-
	TP53	281D>Y	Substitution	Nonsynonymous coding	-
	SMAD4	363C>S	Substitution	Nonsynonymous coding	-
	GNAS	160R>C	Substitution	Nonsynonymous coding	-

Table 2

Copy number alterations identified in cell lines.

Cell Line	Gene ID	Mutation Type	Fold Amplification
SKOV3	CDKN2A	Deletion	NA
	ERBB2	Amplification	4.6
OVSAHO	FGFR4	Amplification	3.6
KURAMOCHI	KRAS	Amplification	10.6
	MYC	Amplification	3